Review

Shallow destructive earthquakes

Hongfeng Yang[1,2,✉], and Suli Yao[1,2]

[1] *Earth System Science Programme*, *Faculty of Science*, *The Chinese University of Hong Kong*, *Hong Kong* 999077, *China*
[2] *Shenzhen Research Institute*, *The Chinese University of Hong Kong*, *Shenzhen*, *Guangdong* 518057, *China*

Corresponding author Yang HF, email: hyang@cuhk.edu.hk

Key points:
• Understanding shallow slip in earthquakes is critical as it impacts ground shaking and damage.
• Most earthquakes have shallow slip deficit, yet the mechanism remains controversial.
• Moderate-sized earthquakes nucleating at shallow depths can be quite damaging and are critical in seismic hazard assessment, especially for regions with resource development.

Abstract Depths of earthquake occurrence and large slip distribution are critical for seismic hazard assessment. Numerous examples show that earthquakes with similar magnitudes, however, can result in significantly different ground shaking and damage. One of the critical factors is that whether the large slip was generated near the ground surface. In this article, we reviewed two aspects that are important on this regard, shallow slip deficit and nucleation depth. Understanding how shallow future earthquakes may nucleate in particular regions, such as shale gas fields, is critical for hazard assessment. Whether or not a strong earthquake may slip significantly at shallow depths (less than 3 km) plays crucial rules in seismic hazard preparation and should be further investigated by integrating high-resolution fault zone observations, dynamic rupture simulation, and fault zone properties. Moreover, precisely resolving shallow depth and slip distribution of earthquakes demands InSAR and/or other image data that can better capture the near-fault deformation to constrain the source parameters of earthquakes.

Keywords: shallow earthquake; shallow slip deficit; nucleation depth; seismic hazard assessment.

Citation: Yang HF, and Yao SL (2021). Shallow destructive earthquakes. Earthq Sci **34**(1): 15–23, doi: 10.29382/eqs-2020-0072.

1. Introduction

Earthquakes occur in a variety of depths, from shallow crust to the base of the mantle transition zone. Destructive earthquakes, however, are mostly shallow, concentrating in the upper crust of continents and the shallow portions on the megathrust. Apparently, focal and centroid depths of earthquakes play critical roles in the intensity of ground shaking and thus directly determine the destructing power for earthquakes with similar magnitudes. Understanding what factors determined the depths of large slip is thus critical for seismic hazard assessment. Here we review two aspects from observations: shallow slip of large earthquakes and nucleation depths of moderate-sized earthquakes, and then highlight the significance of identifying and predicting such parameters for future hazard preparation of continental earthquakes.

2. Shallow slip deficit

For shallow earthquakes with magnitudes larger than 6, they are usually very destructive in producing significant damages to the infrastructure and society. However, a number of large continental earthquakes are observed to host the maximum coseismic slip at depths of 3−6 km (Figure 1) (Fialko et al., 2005; Xu XH et al., 2016), leaving a shallow zone of slip deficit. Such shallow slip deficit (SSD) found in large earthquakes is independent of whether the ruptures had extended to the ground. For instance, the 26 December 2003 M_W 6.5 Bam earthquake in southeastern Iran ruptured the fault at depths of 3−7 km with the maximum slip of ~2 m (Fialko et al., 2005). The rupture of this event did not break the surface. While the 1992 M_W 7.3 Landers earthquake in southern California broke the ground but the maximum slip occurred in the

Received 9 December 2020; **received in revised form** 6 January 2021; **accepted** 18 January 2021; **available online** 26 March 2021.

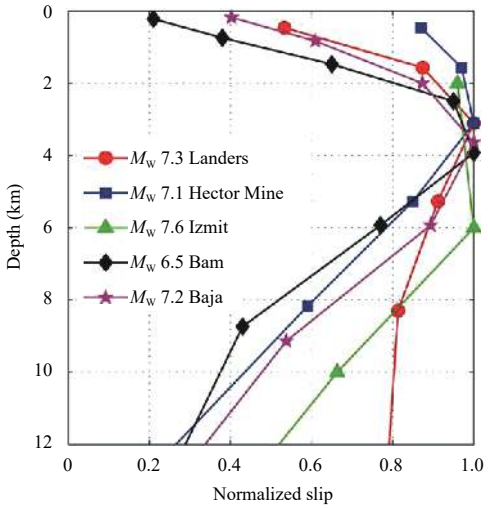

Figure 1. Normalized coseismic slip on the ruptured fault planes of five earthquakes in different tectonic regions that were documented in Fialko et al., (2005) and Kaneko and Fialko (2011). From Kaneko and Fialko (2011).

middle of the seismogenic layer at 4−6 km (Figure 1).

Indeed, the centroid depths of global earthquakes larger than 5.5 show a cluster of ~15 km, despite their different tectonic settings and faulting mechanisms (Figure 2a). Note that the catalog of Global Centroid Moment Tensor (GCMT) may lead to a bias in deeper focal depths of earthquakes, as they fixed the minimum depth of 12 km, probably the reason of the large peak at 15 km (Figure 2a). However, the lack of relatively large earthquakes (e.g. M_W>5) at depths shallower than 3 km is also reflected from other catalogs, in which moment tensor solutions of smaller magnitude earthquakes had been carefully resolved with regional velocity models using the Computer Programs in Seismology (Herrmann, 2013). For earthquakes in North America, most of them are distributed below ~7 km in the upper crust (Figure 2b). In Yunnan, southwest China, centroid depths of earthquakes exhibit concentrations around 10 km (Figure 2c) (Xu Y et al., 2020). Although sporadic shallow earthquakes (e.g. less than 3 km) were reported in both catalogs, there is no doubt that accumulated coseismic slip occurs significantly below 5 km (Figure 2b and 2c).

Efforts have been made to quantitatively understand the source mechanism of the SSD. It has been suggested that the SSD was possibly compensated by shallow creep or afterslip on faults (Scholz, 1998). Although steady-state shallow creep was observed in certain fault segments, e.g. the southern section of the San Andreas Fault (Lyons and Sandwell, 2003) and a few faults in central California (Schulz et al., 1982), most faults have not been observed with shallow creep during interseismic period. Furthermore, geodetic observations indicate that afterslip was too low to account for the SSD generated in a few earthquakes (e.g. Fialko, 2004; Fialko et al., 2005). Therefore, neither shallow creep nor afterslip could be the source of the SSD.

Alternatively, the SSD has been attributed to shallow compliant fault zones that accommodate a distributed inelastic deformation within the uppermost few kilometres of the crust during the interseismic period (Fialko et al., 2005). The compliant fault zones may yield plastically during coseismic ruptures, leading to distributed off-fault inelastic deformation and thus compensating for the SSD. Such mechanism has been investigated by dynamic rupture simulations in both 2D (Kaneko and Fialko, 2011) and 3D models (Roten et al., 2017), in which the predicted degrees of the SSD were close to observations. Such

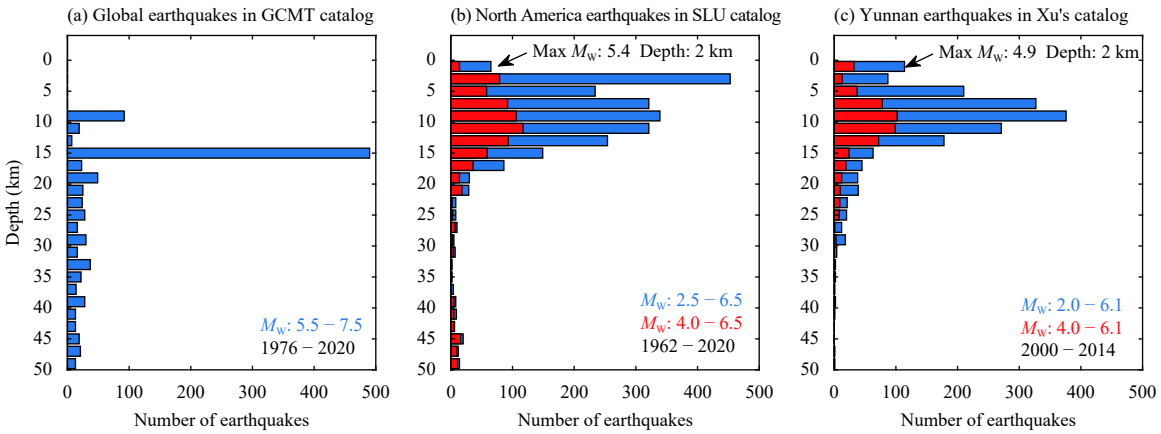

Figure 2. Centroid depth distribution of global earthquakes (a) with moment magnitudes between 5.5 and 7.5, from 1976 to December 2020. Source from Global Centroid Moment Tensor (GCMT) catalog. (b) Earthquakes in North America from the moment tensor catalog in Saint Louis University (SLU; http://www.eas.slu.edu/eqc/eqcquakes.html, last accessed Dec. 30, 2020). (c) Earthquakes from 2000 to 2014 in Yunnan, China, from Xu Y et al., (2020).

compliant fault zones have been documented by geodetic and seismic data, in particular along the fault zones ruptured during the 1992 Landers (Li YG et al., 1994; Peng ZG et al., 2003; Li HY et al., 2007) and 1999 Hector Mine earthquakes (Li YG et al., 2002), which both produced significant SSD (Fialko et al., 2005; Xu XH et al., 2016). Moreover, the compliant fault zones are seismically characterized as low velocity zones that had been found along a number of continental faults (Ben-Zion and Sammis, 2003; Cochran et al., 2009; Yang HF et al., 2011; Ma C et al., 2020; Tian FF et al., 2020; Yang HF et al., 2010; Yang HF et al., 2014; Yang HF, 2015; Yang HF et al., 2020a).

However, the low velocity zones (LVZ) at shallow depths associated with seismogenic faults have been suggested to promote rupture extents in 3D dynamic rupture simulations, although the ruptures did not extend into the LVZ (Weng HH et al., 2016). If the rupture extends to the surface, slip at shallow depths becomes larger on the shallow portion of the fault that was surrounded by the compliant materials with smaller rigidity (Figure 3). Note that such conclusions were drawn based on the assumption of elastic response of the LVZ during coseismic ruptures (Weng HH et al., 2016; Chen X and Yang HF, 2020). When considering inelastic off-fault response in a 2D model, final slip on the fault was also promoted by the presence of the LVZ and the slip increased with the LVZ width (Duan BC, 2008). Therefore, it demands further investigations how the shallow compliant fault zone materials impact on rupture propagation and slip distribution. In particular, how to quantify the degree of plastic yielding of off-fault materials at shallow depths and how they may alter the slip distribution near surface are critical to precisely predict shallow slip distribution in future earthquakes along continental faults.

Furthermore, precisely resolving shallow slip behaviors requires extensive geodetic observations close to the surface rupture. In addition, the estimate of SSD may be discrepant among models with different geodetic datasets or other critical model inputs such as the fault geometry. For instance, the SSD of the 1992 Landers M_W 7.3 earthquake was originally reported to be ~ 50% in the slip model (Figure 1) that was inversed from the GPS data and InSAR data (Fialko, 2004). While a recent study (Xu XH et al., 2016), which revisits this event by further incorporating the optical imagery data and the SAR azimuth offsets, indicates a much smaller degree (20%) of the SSD (Figure 4a). Similarly, smaller SSDs are inferred for the Hector Mine M_W 7.1 and the El Mayer-Cucapah M_W 7.2 earthquakes after adding more geodetic data and more detailed processing into the inversions (Figure 4a) (Xu XH et al., 2016). Advances in the near-fault geodetic measurements are critical in precisely constraining the SSD.

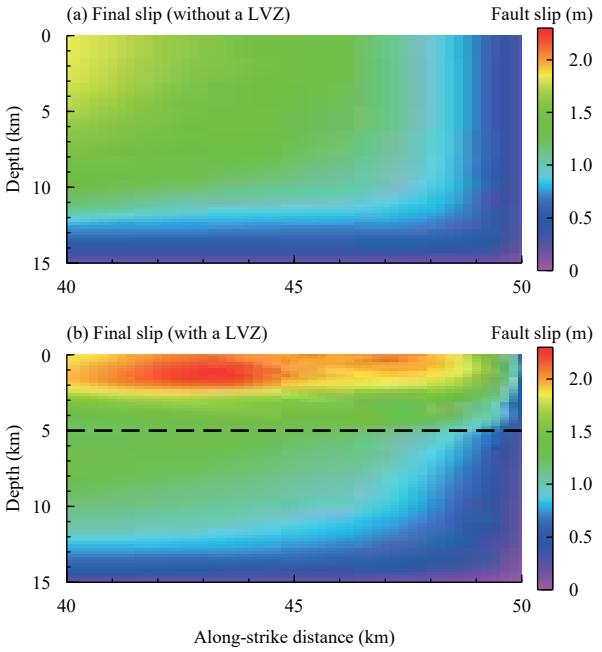

Figure 3. Final slip distribution on the fault plane from dynamic rupture simulations. (a) Without a low velocity zone (LVZ); (b) with a LVZ extending to 5 km (dashed line). Modified from Chen X and Yang HF (2020).

In stark contrast, some earthquakes apparently do not exhibit such SSD and may significantly break the ground surface. For instance, the 3 August 2014 M_W 6.2 Ludian earthquake ruptured the conjugate Zhaotong-Ludian fault system (Zhang GW et al., 2014), with the maximum slip of 1.6 m near the surface on the NNW-SSE oriented fault plane (Niu YF et al., 2020). Although slip distribution and the maximum slip differ in kinematic rupture models that were constrained from different data (Liu CL et al., 2014; Zhang Y et al., 2015), it is consistent that the maximum slip occurred near surface (Figure 4b), one of the reasons leading to severe damages during the 2014 Ludian earthquake. Furthermore, the 14 April 2010 M_W 6.9 Yushu earthquake produced a maximum slip of 2.0 m at 3-km depth, with > 1.5 m slip near the ground surface on the Jiegu segment (Wen Y et al., 2013). Although details of slip distribution were slightly different, the characteristic of significant slip (~ 1 m) near the ground was consistent among different source models of the Yushu earthquake that were constrained from satellite images (Figure 4b) (Jiang GY et al., 2013; Tobita et al., 2011; Wang XW et al., 2014). Whether coseismic ruptures extend to the ground surface is critical for seismic hazard. Therefore,

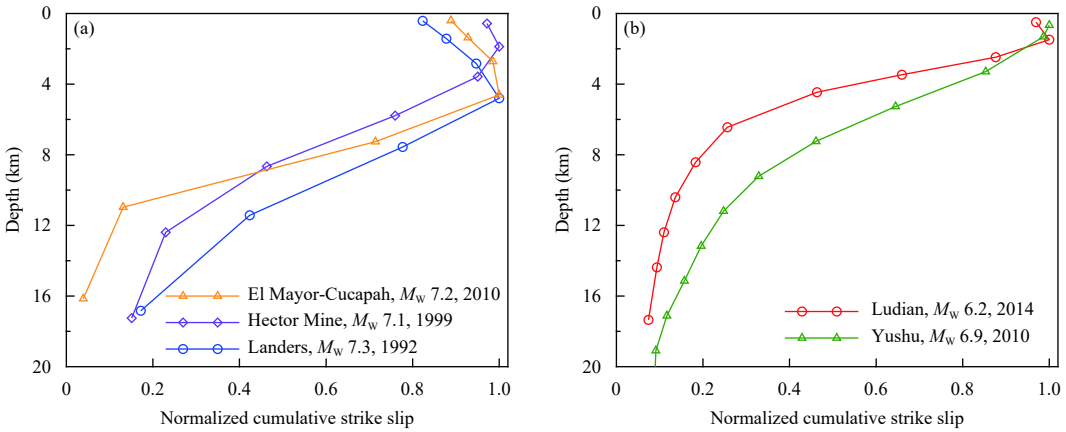

Figure 4. (a) Normalized cumulative slip averaged along strike for the 1992 M_W 7.3 Landers, 1999 M_W 7.1 Hector Mine, and 2010 M_W 7.2 El Mayor-Cucapah earthquakes, after re-processing near-field deformation data (Xu XH et al., 2016). (b) Normalized cumulative average slip for the 2010 M_W 6.9 Yushu and 2014 M_W 6.2 Ludian earthquakes, showing no shallow slip deficit. From source models of Jiang GY et al., (2013) and Niu YF et al., (2020), respectively.

investigating what determined such behavior of earthquake ruptures is demanded with high priority.

3. Nucleation depths of moderate-sized earthquakes

In addition to the SSD produced by large continental earthquakes, one important factor is how shallow earthquakes nucleate, because even a moderate-sized earthquake at very shallow depth can be quite damaging. Numerous reports show that large earthquakes do not nucleate at shallow depths. Based on spontaneous rupture models, Das and Scholz (1983) have suggested that ruptures initiating at greater depths, an environment that is anticipated to have larger stress drop, can propagate over the entire fault plane. In contrast, the ruptures starting from shallow depths where frictional strength and stress drop are smaller are inhibited due to the insufficient strain energy (Das and Scholz, 1983). Although frictional strength may not necessarily increase with depth from dynamic rupture modeling results with near-field constraints (Weng HH and Yang HF, 2018; Yao SL and Yang HF, 2020), it is indeed rare to observe very shallow focal depths of large earthquakes.

It is understood from low-velocity rock sliding experiments that rock samples under conditions representing depths shallower than 2−3 km generally exhibit velocity strengthening (VS), i.e. frictional resistance increases with slip rate, unfavorable for fault acceleration (Blanpied et al., 1998; He CR et al., 2007). Therefore, these areas are anticipated with aseismic slip while in contrast earthquakes should only occur in velocity weakening (VW) conditions, which correspond to upper crust (Scholz, 1998). It is, however, recognized that the VS zones may be broken due to a large rupture nucleated in nearby VW regions (Kaneko et al., 2010; Yang HF et al., 2012). But ruptures would not nucleate within the VS region by themselves.

However, reports have shown that moderate-to-large magnitude earthquakes do occur at very shallow depths, some of which became quite destructive. By analysis of depth phases such as sP and Rg of foreshocks and aftershocks of the 1968 M_S 6.8 Meckering, west Australia, earthquake, Langston (1987) suggested that the foreshocks were located mostly at less than 2 km depth and most aftershocks occurred within 1 km of the surface, consistent with a previous study of the mainshock based on teleseismic waveforms. The locations of foreshocks and aftershocks implied that the mainshock rupture initiated at depth of 2 km and propagated downward to 7 km, which was inferred from the maximum depth of aftershocks (Langston, 1987). Such shallow nucleation depth and downward propagation of rupture marked the 1968 M_S 6.8 Meckering event a very rare earthquake, plausibly a result of high strength in the cold shield crust.

Such shallow earthquakes were not only reported in intraplate shield, but also along major block boundaries. In the northeastern end of the rupture zone of the 12 May 2008 M_W 7.9 Wenchuan earthquake, a M_S 5.7 aftershock occurred at Qingchuan on 24 July 2008. Based on waveform modeling of sPL phases of its aftershocks, they were located at depth less than 3 km (Luo Y et al., 2010). In addition, the well-developed Rayleigh wave of the M_S 5.7 earthquake recorded at a station within 15 km of epicentral distance implied a focal depth of no more than

3 km (Luo Y et al., 2010). Such shallow earthquakes were attributed to stress increase from the deep coseismic slip during the 2008 M_W 7.9 Wenchuan earthquake.

More recently, on 11 August 2016, a M_W 4.1 thrust earthquake occurred in the Eastern Sichuan Basin and led to three injuries, in a region with historically low seismicity. Seismic waveform modeling constrained the centroid depth of this event to be 1 km, which was consistent with ground deformation that was captured by InSAR data. This event was interpreted to be induced by removal of 10 m thick surface rock layer during the construction (Qian YY et al., 2019).

Moreover, a shallow earthquake with M_W 4.3 occurred on 25 February 2019, in the shale gas field of Rongxian, Sichuan. This earthquake was constrained by InSAR and seismic data to have a centroid depth of 1 km on the Molin fault (Figure 5), one of the major reasons for this earthquake to be very destructive (Yang HF et al., 2020b). Two fatalities and 12 injuries were caused by the M_W 4.3 Rongxian earthquake, despite its relatively small magnitude. Analysis of spatial and temporal correlation between the earthquake and nearby hydraulic fracturing wells suggests a possible causal relationship. But it remains enigmatic why such a shallow fault was activated to slip coseismically (Yang HF et al., 2020b; Wang MM et al., 2020). The host rocks of the Molin fault are marlstone and limestone. According to results of laboratory frictional experiments on sedimentary rock samples (mudstone, sandstone, limestone) from the Sichuan Basin, all samples under conditions representing shallow depths (< 2 km) exhibit VS behavior (Verberne et al., 2010), and thus are anticipated to slip aseismically. The shallow 2019 February M_W 4.3 earthquake apparently challenges such traditional view and raises a significant question of how to evaluate potential seismic hazard and risks for hydraulic fracturing near very shallow faults. It is also demanded to further investigate the probability of coseismic slip on very shallow faults.

Accompanying the occurrence of shallow damaging earthquakes, challenges arise in resolving earthquake source parameters, especially in focal depths, which are important in elucidating mechanisms of why such earthquakes occurred. For instance, the focal depth of the 2019 February M_W 4.3 Rongxian earthquake was suggested to be ~2 km (Lei XL et al., 2020; Yi GX et al., 2020), slightly greater than the results in Yang HF et al., (2020b). In general, such small difference would not matter much for earthquakes occurring below 5 km. However, the precise depth estimation becomes critical for shallow earthquakes, e.g. the 2019 Rongxian earthquake, because the Molin fault was found terminating at a depth of ~1.5 km (Figure 5b) (Wang MM et al., 2020). Focal depths with large uncertainties may lead to problematic interpretation of source faults in the region.

In addition, the focal depths of the two largest earthquakes in the Weiyuan Shale Gas Field (WSGF) are in debate, probably due to the limited station coverage. On September 8, 2019, a M_W 5.0 earthquake occurred in the east cluster to Weiyuan. Using the crust 1.0 velocity model, Wang MM et al., (2020) constrained the focal depth at 5 km, close to the result (4.5 km) using another velocity model that was derived from relocated local

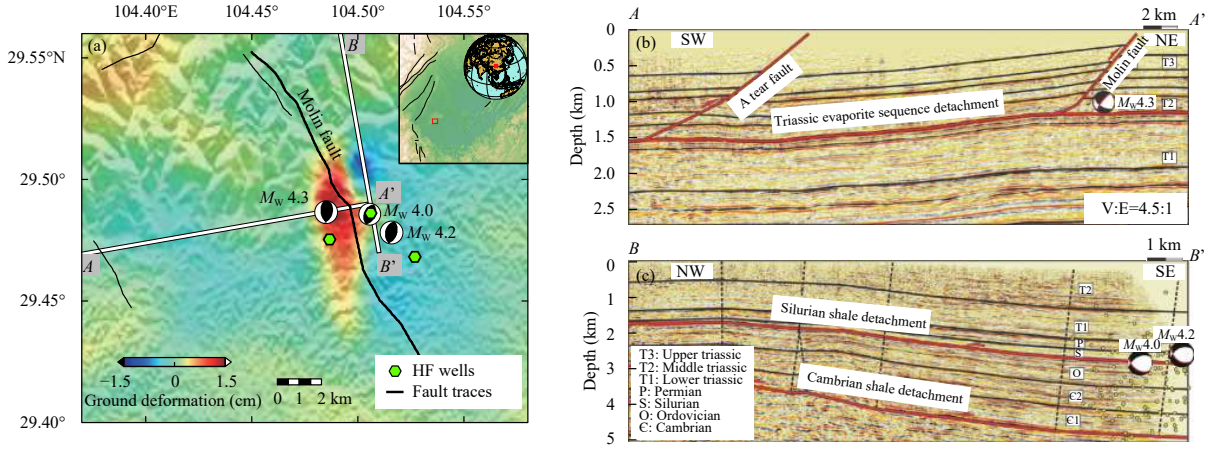

Figure 5. (a) InSAR image (line of sight direction: southeast) of ground deformation caused by the 2019 February M_W 4.3 earthquake (Yang HF et al., 2020b). Black traces denote faults. Green hexagons show locations of hydraulic fracturing (HF) wells. The beach balls indicate the focal mechanisms for the mainshock and the two foreshocks (Yang HF et al., 2020b). (b) and (c) Seismic reflection profiles along the two profiles *AA*' and *BB*' (panel a). Cross section *AA*' is vertically exaggerated (×4.5). Modified from Figure 5 in Wang MM et al. (2020).

earthquakes (Yi GX et al., 2020). However, two other studies resolved its focal depth at 2.5 km (Lei XL et al., 2020) and 2.9 km (Sheng et al., 2020), respectively, which were slightly shallower than the injection depth (3.0 km). Similarly, the focal depths of the 18 December 2019 M_W 4.9 earthquake differed from 4 km (Yi GX et al., 2020), 3 km (Sheng et al., 2020), to 2.5 km (Lei XL et al., 2020). Resolving earthquake source parameters in high resolution is necessary to infer whether and how these earthquakes were induced by fracking activities in the WSGF.

4. Discussion and future directions

Although most large earthquakes nucleate in the middle or near the base of the seismogenic zone and leave the SSD, there are exceptional cases of causing large slip at very shallow depth and thus leading to severe ground shaking and damage, as discussed in above examples of the 2010 M_W 6.1 Yushu and 2014 M_W 6.9 Ludian earthquakes. Evaluating whether or not large shallow slip may occur along continental faults is thus necessary for future seismic hazard assessment. Indeed, earthquake rupture propagation is a complex nonlinear process that is governed by a number of factors. Heterogeneities of fault zone properties, including fault zone materials (e.g. Duan BC, 2008; Harris and Day, 1997; Weng HH et al., 2016), fault geometry (e.g. Yang HF et al., 2013; Yu HY et al., 2018), stress distribution and frictional properties (e.g. Weng HH et al., 2015; Weng HH and Yang HF, 2018; Yao SL and Yang HF, 2020), play critical roles in slip distribution. Although stress condition on seismogenic faults remains elusive, various lines of evidence indicate that stress distribution on faults is heterogeneous. As a result, ruptures initiating at different positions on the fault plane may result in distinctly different rupture extent and slip distribution (Yang HF et al., 2019), making it more challenging to predict potential shallow slip in future earthquakes. Integrating seismological observations on fault zones, frictional properties of rock samples representing shallow faults, and dynamic mechanism of rupture propagation is desired to better tackle such a challenging problem.

On the other hand, accurately resolving focal depths of shallow earthquakes is not only critical for elucidating tectonic setting and potential inducing mechanisms of faulting, but also holds important implications for earthquake emergency response. As shown in the case of 8 September 2019 M_W 5.0 earthquake in Weiyuan, it is controversial to resolve the centroid depth using conventional seismological techniques, whose resolutions are subject to station coverage, frequency band of waveforms, and imperfect velocity models. Indeed, the residual difference in waveform-based seismological solutions such as from the gCAP method (Zhu LP and Ben-Zion, 2013) may not be that distinct for shallow earthquakes. For instance, the misfit values of focal depths at 1 km and 2 km for the 2019 Febuary M_W 4.3 Rongxian earthquake are quite close (Yang HF et al., 2020b). Even results of forward waveform modeling show subtle changes in synthetic waveforms at most stations, including the closest one that was 13.5 km in distance (Figure 6). Therefore, resolving accurate depths of shallow earthquakes demands additional constraints.

Detailed analysis of depth phases such as sPL and sP is very helpful to constrain the earthquake depth (e.g. Langston, 1987; Luo Y et al., 2010), but is usually subject to station coverage and data quality. In contrast, InSAR data has been proven very effective to constrain the depths of shallow moderate-magnitude earthquakes (e.g. Qian YY et al., 2019; Yang HF et al., 2020b). Since the application on the 1992 Landers earthquake (Massonnet et al., 1994), InSAR data have been extensively used to constrain co-, inter-, and post-seismic deformation of numerous large continental earthquakes. In addition to focal depths, it has also been well noted that constraining slip distribution jointly from InSAR and seismic data can significantly improve the resolution and robustness in kinematic source models (Yue H et al., 2020). Incorporating InSAR data to constrain source parameters of earthquakes is very helpful to precisely resolve shallow depth and slip distribution of earthquakes.

Although moderate earthquakes usually produced little damage, they may become destructive if they occur at shallow depths, as evidenced by recent earthquakes in the Sichuan Basin (Qian YY et al., 2019; Yang HF et al., 2020b; Sheng et al., 2020). Even though M4 earthquakes may not occur that often, earthquakes with smaller magnitudes (e.g. 3) may be frequent and can cause damage to underground infrastructure, such as underground gas storage (Zhou PC et al., 2019; Jiang GY et al., 2020), CO_2 sequestration (Zoback and Gorelick, 2012), and horizontal wells to conduct hydraulic fracturing during shale gas development. In addition to small earthquakes, aseismic slip may also lead to damage to the infrastructure. For instance, casing distortion in the Shale Gas Fields at Sichuan Basin is severe (Xie J, 2018), and it is unclear whether the distortion was caused by earthquakes or aseismic slip. Understanding the fault slip at shallow depths in a full spectrum spanning from long-term and episodic creep, slow slip events, and earthquakes is

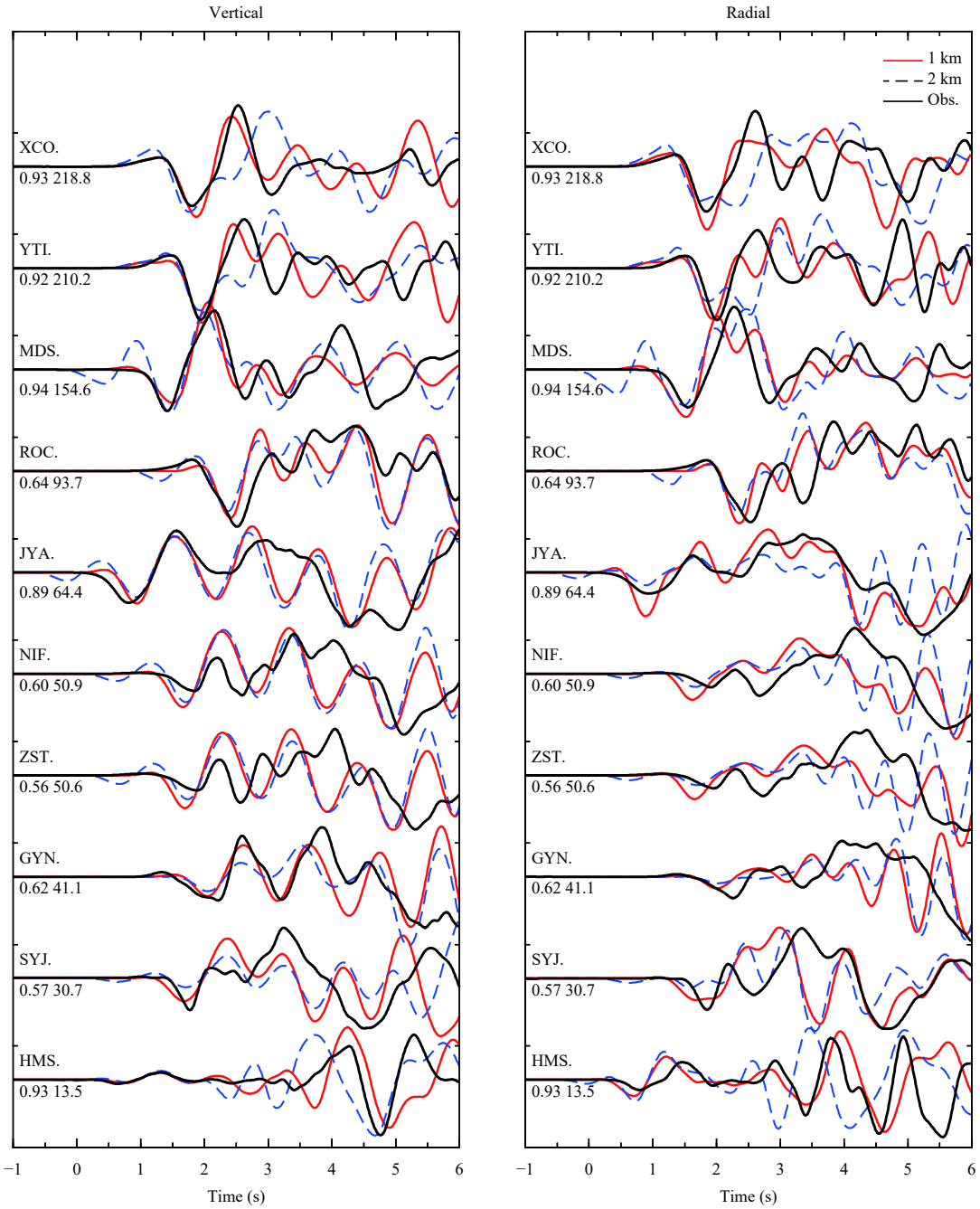

Figure 6. Waveform comparison of synthetics with the data (black) on the vertical (left) and radial (right) components for the 2019 Febuary M_W 4.3 Rongxian earthquake at 1 (red) and 2 km (blue) depths, respectively. Station names, waveform cross correlation coefficient, and epicentral distance (in km) are marked for each station.

necessary not only for advancing our understanding of faulting mechanics and earthquake hazard preparation, but also holds critical keys to prevent underground infrastructure from potential failure and damage.

Acknowledgments

This work was supported by National Key R&D Program of China (No. 2018YFC1503400), China Earthquake Science Experiment Project, CEA (Nos. 2018CSES0101, 2018CSES0102, and 2019CSES0107), Hong Kong Research Grant Council Grants (Nos. 14306418, and 14304820), NSFC/RGC Joint Scheme (N_CUHK430/16), and Faculty of Science at CUHK. The authors thank Dr. Pengcheng Zhou and Miss Xiang Chen for help produce the figures.

References

Ben-Zion Y, and Sammis CG (2003). Characterization of fault zones. Pure Appl Geophys **160**: 677–715.

Blanpied ML, Marone CJ, Lockner DA, Byerlee JD, and King DP (1998). Quantitative measure of the variation in fault rheology due to fluid-rick interactions. J Geophys Res: Solid Earth **103**(B5): 9691–9712.

Chen X, and Yang HF (2020). Effects of seismogenic width and low-velocity zones on estimating slip-weakening distance from near-fault ground deformation. Geophys J Int **223**(3): 1497–1510.

Cochran ES, Li YG, Shearer PM, Barbot S, Fialko Y, and Vidale JE (2009). Seismic and geodetic evidence for extensive, long-lived fault damage zones. Geology **37**(4): 315–318.

Das S, and Scholz CH (1983). Why large earthquakes do not nucleate at shallow depths. Nature **305**(13): 621–623.

Duan BC (2008). Effects of low-velocity fault zones on dynamic ruptures with nonelastic off-fault response. Geophys Res Lett **35**(4): L04307.

Fialko Y (2004). Evidence of fluid-filled upper crust from observations of postseismic deformation due to the 1992 M_W 7.3 Landers earthquake. J Geophys Res **109**: B08401.

Fialko Y, Sandwell D, Simons M, and Rosen P (2005). Three-dimensional deformation caused by the Bam, Iran, earthquake and the origin of shallow slip deficit. Nature **435**: 295–299.

Jiang GY, Xu CJ, Wen YM, Liu Y, Yin Z, and Wang JJ (2013). Inversion for coseismic slip distribution of the 2010 M_W 6.9 Yushu Earthquake from InSAR data using angular dislocations. Geophys J Int **194**(2): 1011–1022.

Harris RA, and Day SM (1997). Effects of a low-velocity zone on a dynamic rupture. Bull Seismol Soc Amer **87**(5): 1267–1280.

He CR, Wang ZL, and Yao WM (2007). Frictional sliding of gabbro gouge under hydrothermal conditions. Tectonophysics **445**(3-4): 353–362.

Herrmann RB (2013). Computer programs in seismology: An evolving tool for instruction and research. Seism Res Lettr **84**: 1081–1088.

Jiang GY, Qiao XJ, Wang XQ, Lu RQ, Liu L, Yang HF, Su YD, Song LL, Wang BS, and Wong TF (2020). GPS observed horizontal ground extension at the Hutubi (China) underground gas storage facility and its application to geomechanical modeling for induced seismicity. Earth Planet Sci Lett **530**: 115943.

Kaneko Y, and Fialko Y (2011). Shallow slip deficit due to large strike-slip earthquakes in dynamic rupture simulations with elasto-plastic off-fault response. Geophys J Int **186**(3): 1389–1403.

Kaneko Y, Avouac JP, and Lapusta N (2010). Towards inferring earthquake patterns from geodetic observations of interseismic coupling. Nat Geosci **3**: 363–369.

Langston CA (1987). Depth of faulting during the 1968 Meckering, Australia, earthquake sequence determined from waveform analysis of local seismograms. J Geophys Res: Solid Earth **92**(B11): 11561–11574.

Lei XL, Su JR, and Wang ZW (2020). Growing seismicity in the Sichuan Basin and its associated with industrial activities. Sci China Earth Sci **63**(11): 1633–1660.

Li HY, Zhu LP, and Yang HF (2007). High-resolution structures of the Landers fault zone inferred from aftershock waveform data. Geophys J Int **171**: 1295–1307.

Li YG, Aki K, Adams D, Hasemi A, and Lee WHK (1994). Seismic guided waves trapped in the fault zone of the Landers, California, earthquake of 1992. J Geophys Res **99**(B6): 11705–11722.

Li YG, Vidale JE, Day SM, Oglesby DD, and SCEC Field Working Team (2002). Study of the 1999 M 7.1 Hector Mine, California, earthquake fault plane by trapped waves. Bull Seismol Soc Amer **92**(4): 1318–1332.

Liu CL, Zheng Y, Xiong X, Fu R, Shan B, and Diao FQ (2014). Rupture process of M_S 6.5 Ludian earthquake constrained by regional broadband seismograms. Chin J Geophys **57**(9): 3028–3037 (in Chinese with English abstract).

Luo Y, Ni SD, Zeng XF, Zheng Y, Chen QF, and Chen Y (2010). A shallow aftershock sequence in the north-eastern end of the Wenchuan earthquake aftershock zone. Sci China Earth Sci **53**(11): 1655–1664.

Lyons S, and Sandwell D (2003). Fault creep along the southern San Andreas from interferometric synthetic aperture radar, permanent scatterers, and stacking. J Geophys Res **108**(B1): 2047.

Ma C, Lei JS, and Xu XW (2020). Three-dimensional shear-wave velocity structure under the Weifang segment of the Tanlu fault zone in eastern China inferred from ambient noise tomography with a short-period dense seismic array. Phys Earth Planet Inter **309**: 106590.

Massonnet D, Feigl K, Rossi M, and Adragna F (1994). Radar interferometric mapping of deformation in the year after the Landers earthquake. Nature **369**(6477): 227–230.

Niu YF, Wang S, Zhu W, Zhang Q, Lu Z, Zhao CY, and Qu W (2020). The 2014 M_W 6.1 Ludian earthquake: the application of RADARSAT-2 SAR interferometry and GPS for this conjugated ruptured event. Remote Sens **12**(1): 99.

Peng ZG, Ben-Zion Y, Michael AJ, and Zhu LP (2003). Quantitative analysis of seismic fault zone waves in the rupture zone of the Landers, 1992: California earthquake: evidence for a shallow trapping structure. Geophys J Int **155**: 1021–1041.

Qian YY, Chen XF, Luo H, Wei SJ, Wang T, Zhang ZG, and Luo XY (2019). An extremely shallow M_W4.1 thrust earthquake in the eastern Sichuan Basin (China) likely triggered by unloading during infrastructure construction. Geophys Res Lett **46**(23): 13775–13784.

Roten D, Olsen KB, and Day SM (2017). Off-fault deformations and shallow slip deficit from dynamic rupture simulations with fault zone plasticity. Geophys Res Lett **44**: 7733–7742.

Scholz CH (1998). Earthquakes and friction laws. Nature **391**: 37–42.

Schulz SS, Mavko GM, Burford RO, and Stuart WD (1982). Long-term fault creep observations in central California. J Geophys Res **87**(B8): 6977–6982.

Sheng MH, Chu RS, Ni SD, Wang Y, Jiang LM, and Yang HF (2020). Source parameters of three moderate size earthquakes in Weiyuan, China, and their relations to shale gas hydraulic

fracturing. J Geophys Res: Solid Earth **125**: e2020JB019932.
Tian FF, Lei JS, and Xu XW (2020). Teleseismic P-wave crustal tomography of the Weifang segment on the Tanlu fault zone: A case study based on short-period dense seismic array experiment. Phys Earth Planet Inter **306**: 106521.
Tobita M, Nishimura T, Kobayashi T, Hao KX, and Shindo Y (2011). Estimation of coseismic deformation and a fault model of the 2010 Yushu earthquake using PALSAR interferometry data. Earth Planet Sci Lett **307**(3-4): 430–438.
Verberne BA, He CR, and Spiers CJ (2010). Frictional properties of sedimentary rocks and natural fault gouge from the Longmen Shan fault zone, Sichuan, China. Bull Seism Soc Amer **100**(5B): 2767–2790.
Wang MM, Yang HF, Fang LH, Han LB, Jia D, Jiang DQ, and Yan B (2020). Shallow faults reactivated by hydraulic fracturing: The 2019 Weiyuan earthquake sequences in Sichuan, China. Seismo Res Lett **91**(6): 3171–3181.
Wang XW, Liu GX, Yu B, Dai KR, Zhang R, Chen Q, and Li ZL (2014). 3D coseismic deformations and source parameters of the 2010 Yushu earthquake (China) inferred from DInSAR and multiple-aperture InSAR measurements. Remote Sensing of Environ **152**: 174–189.
Wen Y, Xu C, Liu Y, Jiang G, and He P (2013). Coseismic slip in the 2010 Yushu earthquake (China), constrained by wide-swath and strip-map InSAR. Nat Hazards Earth Syst Sci **13**(1): 35–44.
Weng HH, Huang JS, and Yang HF (2015). Barrier-induced supershear ruptures on a slip weakening fault. Geophys Res Lett **42**(12): 4824–4832.
Weng HH, Yang HF, Zhang ZG, and Chen XF (2016). Earthquake rupture extents and coseismic slips promoted by damaged fault zones. J Geophys Res: Solid Earth **121**(6): 4446–4457.
Weng HH and Yang HF (2018). Constraining frictional properties on fault by dynamic rupture simulations and near-field observations. J Geophys Res: Solid Earth **123**(8): 6658–6670.
Xie J (2018). Practices and achievements of the Changning-Weiyuan shale gas national demonstration project construction. Natur Gas Ind **38**(2): 1–7 (in Chinese with English abstract).
Xu XH, Tong XP, Sandwell DT, Milliner CWD, Dolan JF, Hollingsworth J, Leprince S, and Ayoub F (2016). Refining the shallow slip deficit. Geophys J Int **204**(3): 1867–1886.
Xu Y, Koper KD, Burlacu R, Herrmann RB, and Li DN (2020). A new uniform moment tensor catalog for Yunnan, China, from January 2000 through December 2014. Seismo Res Lett **91**(2A): 891–900.
Yang HF (2015). Recent advances in imaging crustal fault zones: a review. Earthq Sci **28**(2): 151–162.
Yang HF, Li ZF, Peng ZG, Ben-Zion Y, and Vernon F (2014). Low-velocity zones along the San Jacinto Fault, Southern California, from body waves recorded in dense linear arrays. J Geophy Res: Solid Earth **119**(12): 8976–8990.
Yang HF, Zhu LP, and Cochran ES (2011). Seismic structures of the Calico fault zone inferred from local earthquake travel time modelling. Geophys J Int **186**(2): 760–770.
Yang HF, and Zhu LP (2010). Shallow low-velocity zone of the San Jacinto fault from local earthquake waveform modeling. Geophys J Int **183**(1): 421–432.
Yang HF, Liu YJ, and Lin J (2012). Effects of subducted seamounts on megathrust earthquake nucleation and rupture propagation. Geophys Res Lett **39**(24): L24302.
Yang HF, Liu YJ, and Lin J (2013). Geometrical effects of a subducted seamount on stopping megathrust ruptures. Geophys Res Lett **40**(10): 2011–2016.
Yang HF, Yao SL, He B, and Newman AV (2019). Earthquake rupture dependence on hypocentral location along the Nicoya Peninsula subduction megathrust. Earth Planet Sci Lett **520**: 10–17.
Yang HF, Zhou PC, Fang N, Zhu GH, Xu WB, Su JR, Meng FB, and Chu RS (2020b). A shallow shock: the 25 February 2019 M_L 4.9 earthquake in the Weiyuan shale gas field in Sichuan, China. Seismo Res Lett **91**(6): 3182–3194.
Yang HF, Duan YH, SongJH, Jiang XH, Tian XF, Yang W, Wang WT, and Yang J (2020a). Fine structure of the Chenghai fault zone, Yunnan, China, constrained from teleseismic travel time and ambient noise tomography. J Geophys Res: Solid Earth **125**(7): e2020JB019565.
Yao SL, and Yang HF (2020). Rupture dynamics of the 2012 Nicoya M_W 7.6 earthquake: evidence for low strength on the megathrust. Geophys Res Lett **47**(13): e2020GL087508.
Yi GX, Long F, Liang MJ, Zhao M, and Wang SM (2020). Geometry and tectonic deformation of seismogenic structures in the Rongxian-Weiyuan-Zizhong region, Sichuan Basin: insights from focal mechanism solutions. Chin J Geophys **63**(9): 3275–3291 (in Chinese with English abstract).
Yu HY, Liu YJ, Yang HF, and Ning JY (2018). Modeling earthquake sequences along the Manila subduction zone: Effects of three-dimensional fault geometry. Tectonophysics **733**(1): 73–84.
Yue H, Zhang Y, Ge ZX, Wang T, and Zhao L (2020). Resolving rupture processes of great earthquakes: Reviews and perspective from fast response to joint inversion. Sci China Earth Sci **63**(4): 492–511.
Zhang Y, Chen YT, Xu LS, Wei X, Jin MP, and Zhang S (2015). The 2014 M_W 6.1 Ludian, Yunnan, earthquake: A complex conjugated ruptured earthquake. Chin J Geophys **58**(1): 153–162 (in Chinese with English abstract).
Zhang GW, Lei JS, Liang SS, and Sun CQ (2014). Relocations and focal mechanism solutions of the 3 August 2014 Ludian, Yunnan M_S 6.5 earthquake sequence. Chin J Geophys **57**(9): 3018–3027 (in Chinese with English abstract).
Zhou PC, Yang HF, Wang BS, and Zhuang JC (2019). Seismological investigations of induced earthquakes near the Hutubi underground gas storage facility. J Geophys Res: Solid Earth **124**(8): 8753–8770.
Zhu LP, and Ben-Zion Y (2013). Parameterization of general seismic potency and moment tensors for source inversion of seismic waveform data. Geophys J Int **194**(2): 839–843.
Zoback MD, and Gorelick SM (2012). Earthquake triggering and large-scale geologic storage of carbon dioxide. Proceedings of the National Academy of Sciences **109**(26): 10164–10168.